

Research Article

High-Efficiency Crossed-Loop 4G LTE Antenna for All Display Metal-Rimmed Smartphones

Jaehyun Choi¹, Woonbong Hwang¹, Chisang You², Byungwoon Jung²,
and Wonbin Hong³

¹Department of Mechanical Engineering, Pohang University of Science and Technology (POSTECH),
Pohang 37673, Republic of Korea

²LG Electronics Mobile Communications, Seoul 07796, Republic of Korea

³Department of Electrical Engineering, Pohang University of Science and Technology (POSTECH), Pohang 37673, Republic of Korea

Correspondence should be addressed to Wonbin Hong; whong@postech.ac.kr

Received 30 April 2018; Revised 30 June 2018; Accepted 9 July 2018; Published 28 August 2018

Academic Editor: Ikmo Park

Copyright © 2018 Jaehyun Choi et al. This is an open access article distributed under the Creative Commons Attribution License, which permits unrestricted use, distribution, and reproduction in any medium, provided the original work is properly cited.

A symmetrically crossed-loop antenna featuring very high radiation efficiency across the entire LTE frequency bands for metal-rimmed smartphones with only 2 mm ground clearance is proposed, analyzed, and verified. The employment of even and odd modes is utilized to achieve wide bandwidth across 698–960 MHz (low-frequency spectrum), 1710–2170 MHz (middle-frequency spectrum), and 2300–2690 MHz (high-frequency spectrum). Empirical analysis confirms the crossed-loop topology results in a 180° phase shift of the electric current distribution on the ground plane, resulting in enhancement of the radiation resistance. As a result, the devised LTE antenna exhibits more than 48% to 75% total system efficiency across the entire band of interest, which is the highest efficiency reported in literature for metal-rimmed smartphones with extremely small ground clearance.

1. Introduction

The exponential growth of the smartphone industry in the past decade has introduced a series of unprecedented challenges to mobile antenna engineering. Smartphone antennas have continued to evolve in accordance to the increasing demand for multitasking and instant communication. This trend has induced the requirement for highly efficient mobile antennas that can operate in multiple frequency spectrums. In addition, amid the growing popularity of sleek, slender mobile terminals, the utilization of metallic frames and chassis for smartphones have now become the mainstream. While this may be aesthetically pleasing and mechanically more reliable, the adaption of metallic frame introduces severe adverse effects on the radiation properties of mobile antennas. In recent years, there have been numerous efforts to incorporate multiband mobile antennas within smartphones and mobile terminals. Inverted F antenna (IFA) is among the most widely used antenna topologies [1, 2]. Such

IFA-based metal antenna [1] operates in the quarter wavelength resonant modes, which minimize the real estate area for mobile antennas within smartphones. In [2], an IFA operating at 824–960 MHz and 1710–2690 MHz with the ground clearance of 2 mm is presented. However, the total system efficiency in the lower band barely surpasses 40% and features limited bandwidth. Furthermore, the thickness of the metal rim is 7 mm as opposed to the 5 mm in this work. Slot and aperture antennas have also been one of the preferred methodologies for metal-framed smartphone applications. In [3, 4], incisions and slits are formulated in the rear metallic covers of mobile terminals and an additional space and clearance is allocated between the exterior metal and the RF ground of the antenna to ensure sufficient radiation of the aperture. Recently, as consumers increasingly prefer smartphones with larger display panels, the aforementioned space has continued to shrink. This has resulted in new approaches featuring mobile aperture antennas with very narrow clearances [5, 6].

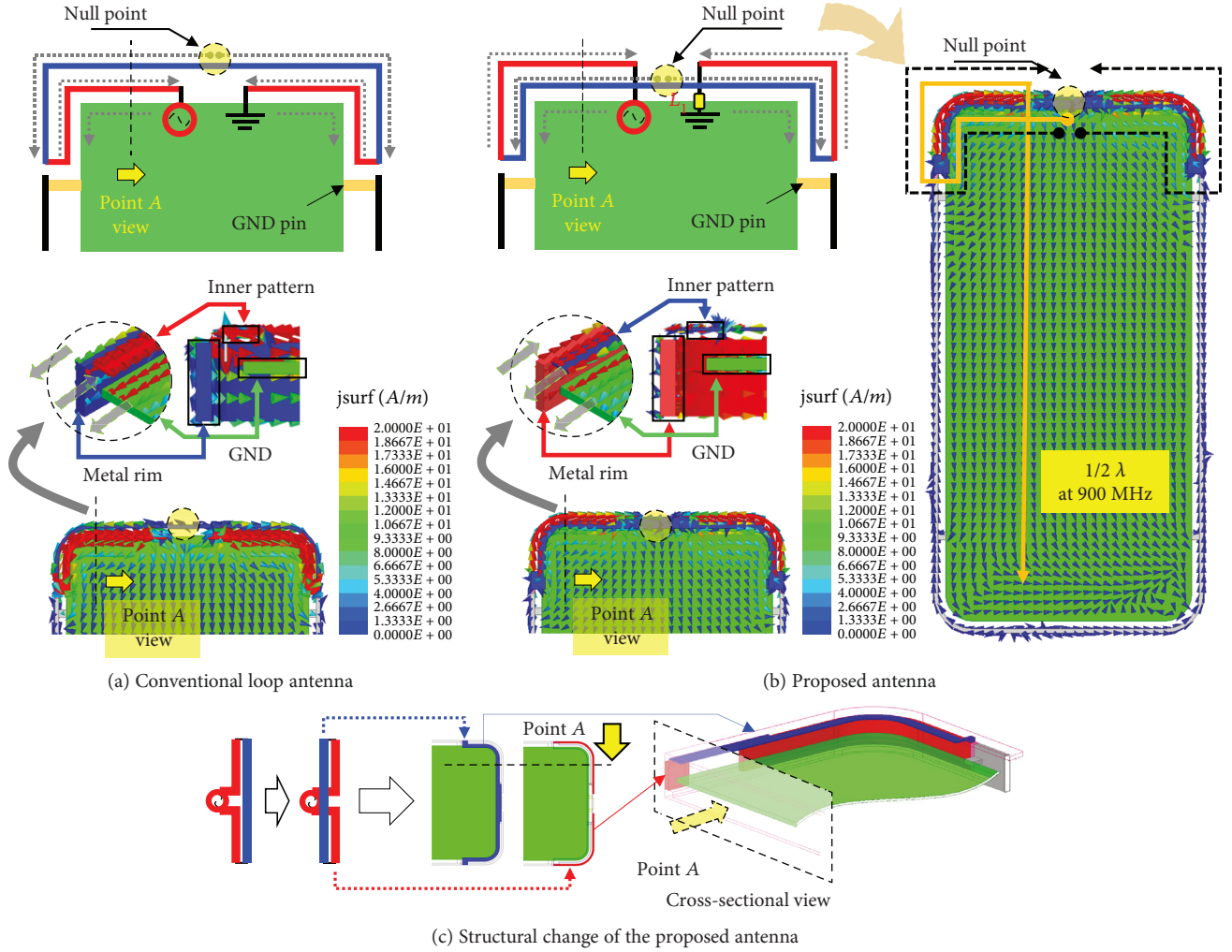


FIGURE 1: Proposed idea and current distribution with a first resonance at 900 MHz in comparison with conventional loop antenna.

The usage of loop topologies for mobile antennas has also been effective. In the past decade, loop antennas have attracted a great deal of attention due to their unique multi-mode characteristics. However, the reported loop antennas [7–9] up to present have collectively been designed in large clearance areas (from 8 mm to 13 mm) which do not accurately reflect modern day smartphone design environments. Moreover, the aforementioned studies have not taken into account of the metallic rim. In [10–13], loop antennas are realized between the metallic rim disposed around the edges of the device and the RF ground. The metallic rim can either be continuous [10, 11] or formulated using numerous gaps or discontinuities [12, 13].

This paper proposes a newly devised mobile antenna topology for metallic smartphones that can operate in the all major frequency spectrums ranging from 698–960 MHz, 1710–2170 MHz, and 2300–2690 MHz [14] while requiring one of the smallest dimensions of 2 mm for the ground clearance ever to be reported in literature. In addition, the featured antenna is designed, fabricated, and characterized using a metallic smartphone prototype and exhibits high efficiencies across the aforementioned frequency bands.

2. Antenna Structure and Principle of Operation

In accordance to the electromagnetic image theory, when an antenna is placed in parallel to a conductor, its radiation characteristics suffer severe degradation due to the out-of-phase electric current [15]. This becomes especially evident when a conventional loop antenna topology is used to formulate an LTE antenna on the edge region of a metal-rimmed smartphone device. As illustrated in Figure 1(a), the close proximity between the loop antenna and the printed circuit board (PCB) ground induces strong return current distribution. As the return current is out-of-phase with the current distribution along the adjacent loop segment, the electromagnetic radiation of the loop antenna is negated in the far field. To mitigate this inherent reduction of radiation resistance, the authors propose a crossed-loop methodology. To minimize the effect of the antenna performance due to the side metal rim structure, the GND pin is applied to the end of the side metal rim facing the end of the loop bent at the corner. As it can be observed in Figure 1(b), the conventional two-dimensional loop antenna is first transformed into a three-dimensional structure by distributing the segments of

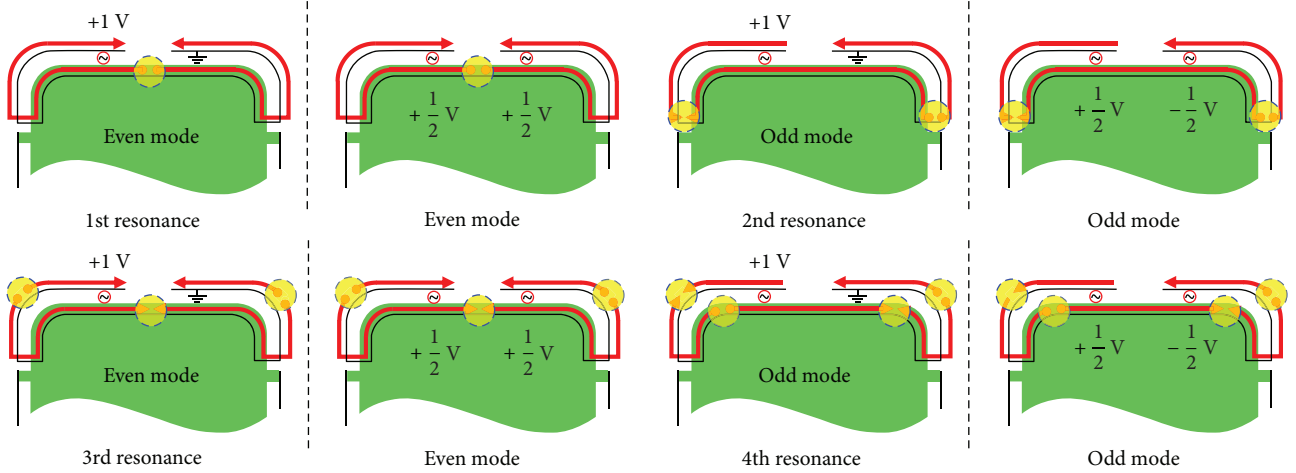


FIGURE 2: Simulated current distribution at each resonance modes for the crossed-loop antenna.

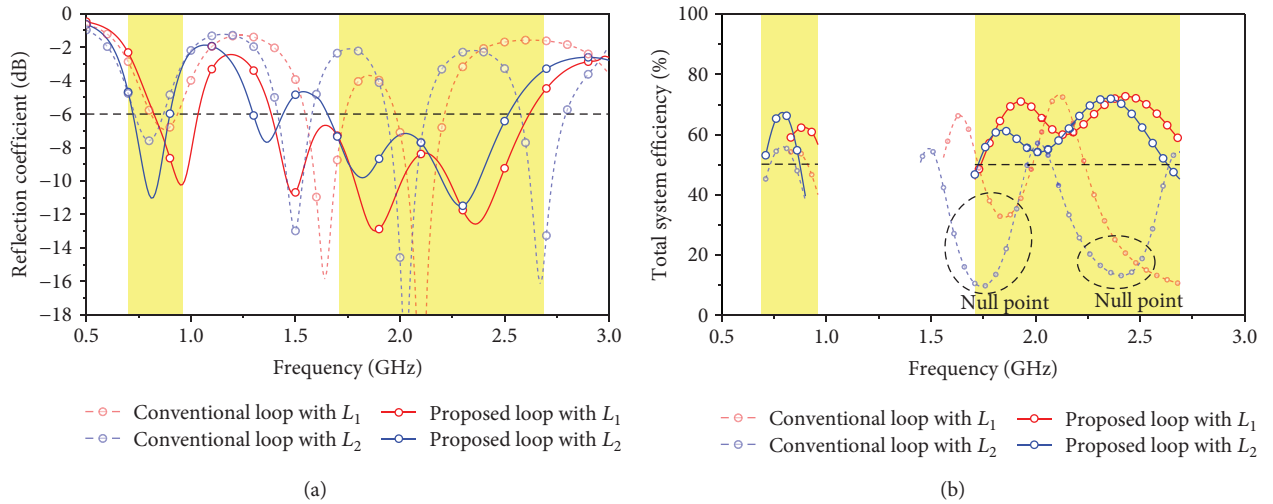


FIGURE 3: Simulated (a) reflection coefficient and (b) total system efficiency of the proposed antenna in comparison with the reference loop antenna.

the loop across two different vertical layers. Afterwards, the cross-loop topology is devised by folding the loop segments of the loop along the outer edge and gradually folding the remaining segments between the outer loop segments and the PCB ground. This introduces two indirect crossings among the loop segments. In this newly devised loop topology, the return current on the PCB is in-phase with the adjacent electric current. In addition, the antenna including the PCB GND is capable of a wideband characteristic with multiple resonance paths as shown in Figure 1(b). The operating principal of the crossed-loop antenna is studied using the mode analysis method to investigate its multiresonance behavior. A similar analytical approach was reported in [16] which explained the method using PIFA with a loaded unfed pin. Illustrated in Figure 2, a half wavelength crossed-loop antenna with a first resonance at 900 MHz is analyzed. By converting the single feed (+1 V) configuration into symmetrical ($+1/2$ V and $+1/2$ V) and asymmetrical ($+1/2$ V and $-1/2$ V), respectively, the resonance mode at 900, 1500,

1900, and 2400 MHz can be analyzed using the even and odd mode analysis. It can be observed that the first and third order resonance operates in the even mode while the second and fourth order resonance functions in the odd mode. For direct comparison with a reference half wavelength loop [17] antenna, a half wave crossed-loop featuring a total length of 169 mm is designed and studied using full-wave numerical simulator ANSYS. For the reference loop antenna and the crossed-loop antenna, each ends of the loop segments are shorted to the PCB using a series inductor. Figure 3(a) presents the comparison of the return loss (S_{11}) conventional loop and the crossed-loop antenna. For each case, two different series inductors of $L_1 = 5$ nH and $L_2 = 15$ nH are applied. The addition of the inductors enables the resonance of the first resonance to shifter lower by an approximate range of 250 MHz. The combination of the even and odd modes is instrumental in enhancing the return loss bandwidth in the case of the proposed antenna topology. Furthermore, it can be ascertained from Figure 3(b) total system

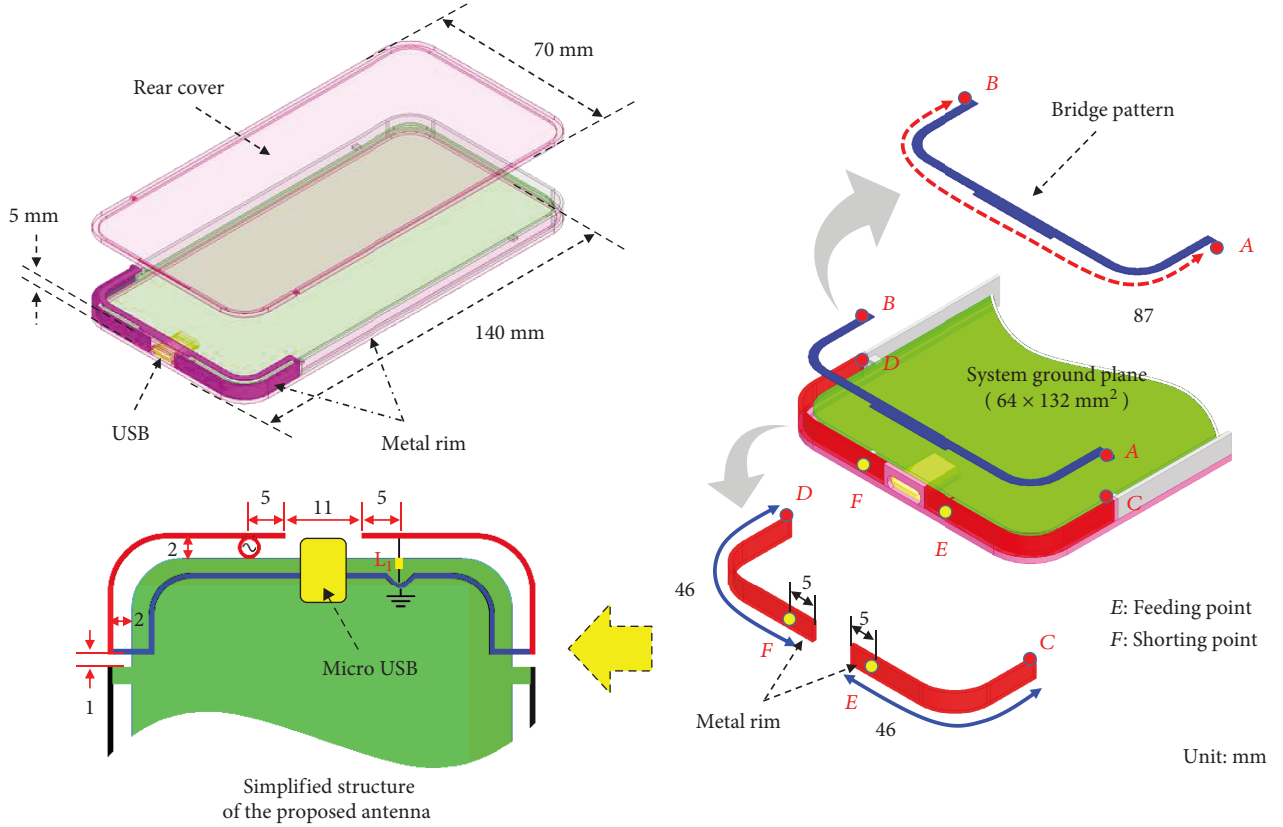


FIGURE 4: Geometry of the proposed antenna with a ground clearance of 2 mm for LTE metal-rimmed smartphone.

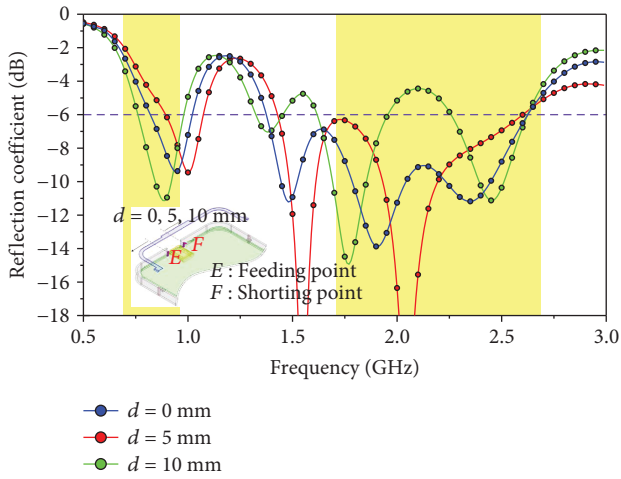


FIGURE 5: Reflection coefficient of the proposed antenna as a function of the feed and short point position (d).

efficiency is significantly improved throughout the three major LTE frequency bands for the crossed-loop design due to the in-phase current distribution in the PCB. On the other hand, under a 2 mm clearance area condition, the return loss characteristics of the conventional loop antenna feature null points resulting in notable total system efficiency degradation.

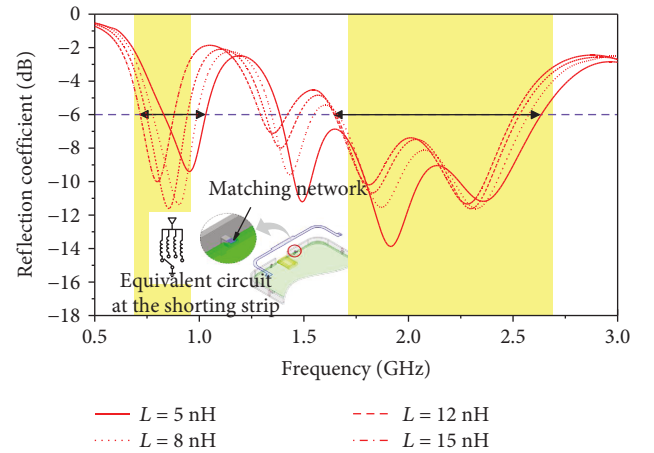


FIGURE 6: Reflection coefficient of the proposed antenna as a function of the inductors.

We proceed by formulating the concept of the half wavelength crossed-loop design into a wideband, high-efficiency LTE antenna for a metal-rimmed smartphone featuring a ground clearance of 2 mm—the smallest dimension ever to be reported in literature. Figure 4 describes the prototype of the LTE smartphone device that will be used in this study. The crossed-loop antenna consists of a bridge pattern disposed on the inner surface of the back cover of the

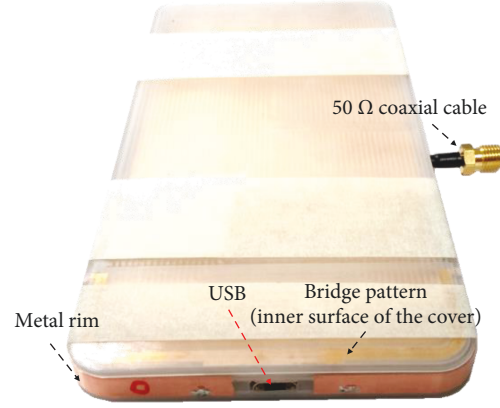


FIGURE 7: Photograph of the fabricated prototype containing the crossed-loop LTE antenna.

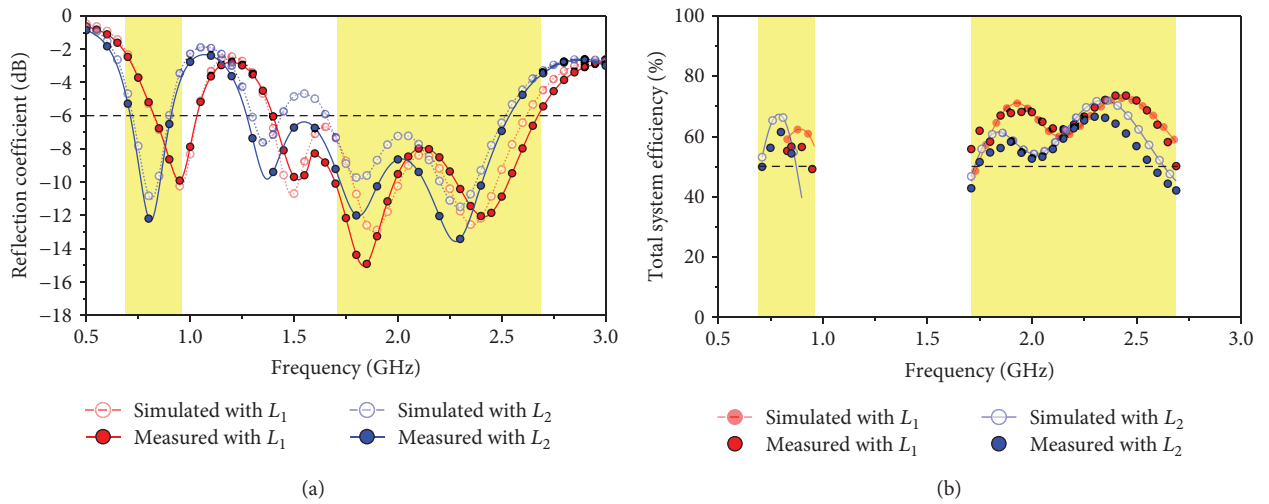


FIGURE 8: Measured and simulated (a) reflection coefficient and (b) total system efficiency of the fabricated crossed-loop LTE antenna inside a metal-rimmed smartphone prototype featuring 2 mm ground clearance.

smartphone prototype and on the vertical face of the metallic rim. The segments comprising the crossed-loop antenna are realized by first establishing an electrical connection between A to C and B to D as shown in Figure 4. One end of the symmetrical crossed-loop antenna is connected to the coaxial feeding network (E) and the other one end of the antenna is shorted to the PCB (F) using a series chip inductor. While points E and F are configured to be 5 mm (d) away from the two open-circuited termination of the loop segment in the final design, their positions can be further modified for precise control of the impedance bandwidth as illustrated in Figure 5. The results as seen in Figure 6 show that the return losses can be controlled to cover the entire LTE low-frequency band by adjusting the inductor applied at the end of shorting strip disposed on the PCB ground plane.

3. Fabrication and Measurement

A metal sheet is used to emulate the metallic frame of the smartphone prototype in the experimental study. The width of the metal frame is configured to be 5 mm to accommodate

the slim profile of today's smartphones. To fine adjust the impedance matching of the antenna during the fabrication process, a rectangular tuning element is protruded at the center of the bridge pattern as presented in Figure 4. This configuration becomes instrumental in case an additional matching network consisting of lumped elements is in need to compensate the return loss deviations caused by fabrication errors. The total ground plane dimension is designed to be $64 \times 132 \text{ mm}^2$ and clearance ground remains at 2 mm. An FR-4 lamination with relative permittivity of 4.4, loss tangent of 0.02, and a thickness of 0.8 mm is used as the PCB substrate.

The finalized crossed-loop antenna features a single coaxial feeding structure to operate in the target LTE frequency band of 698–960 MHz and 1710–2690 MHz. The respective length of the segment along the metallic rim is configured to be 46 mm and 87 mm along the bridge pattern. The fabricated prototype containing the LTE crossed-loop antenna is presented in Figure 7. Two sets of prototypes are realized using different series inductors ($L_1 = 5 \text{ nH}$, $L_2 = 15 \text{ nH}$).

TABLE 1: Comparison of proposed antenna and reference antennas.

Ref.	Metal rim	Electrical component around the antenna	Maximum GND clearance (mm)	Bandwidth (MHz)	Efficiency (%)
[18]	No	No	5 mm	789–900/1680–2740	50–59/52–82
[19]	No	No	10 mm	660–1100/1710–3020	30–65/59–90
[20]	Yes	No	10 mm	824–960/1710–2690	45–60/>47%
[21]	Yes	No	5 mm	824–960/1710–2690	54–96
[22]	Yes	No	8 mm	824–960/1710–2690	>50% 50–78
[2]	Yes	No	2 mm	824–960/1710–2690	40–47/55–78
Proposed	Yes	Yes	2 mm	710–1030/1650–2620	52–65/48–75

Figure 8(a) presents the comparison of the measured and simulated reflection coefficient as function of the series inductance. The total system efficiencies presented in Figure 8(b) indicate that despite the 2 mm ground clearance, the featured antenna exhibits more than 50% total system efficiency throughout the entire LTE frequency band. The additional loss in the measurement is attributed to the ohmic loss of the chip inductors. An overall comparison between the proposed cross-looped LTE antenna for smartphone applications and recent studies is summarized in Table 1. Despite the addition of the metallic rim and extremely small ground clearance, the radiation efficiencies of the presented antenna are quantitatively similar to studies featuring much larger ground clearance dimension.

4. Conclusion

In this study, a symmetrically crossed-loop type antenna integrated inside a metal-rimmed smartphone featuring an extremely small ground clearance of 2 mm has been proposed and studied. The operating principle of the proposed antenna to generate wide operating bands has been presented. The antenna topology consists of metallic frames and a bridge pattern and employs a coaxial feeding network. Agreement between the measured data and simulated results of the proposed antenna has been observed. Switching of the low bands to cover the entire desired lower LTE bands can be controlled by the value of the inductor disposed at one end of the antenna. The optimized antenna is experimentally verified to feature one of the highest total system efficiencies to be reported in literature.

Data Availability

The data used to support the findings of this study are included within the article.

Conflicts of Interest

The authors claim no conflicts of interest.

Acknowledgments

This work was funded and supported by LG Electronics.

References

- [1] J. H. Kim, J.-S. Kim, T.-G. Kim et al., “Antenna using exterior metal frame and electronic device utilizing the same,” U.S. Patent 2016/0064820, 2016.
- [2] K. L. Wong and Y. C. Wu, “Small-size dual-wideband IFA frame antenna closely integrated with metal casing of the LTE smartphone and having decreased user’s hand effects,” *Microwave and Optical Technology Letters*, vol. 58, no. 12, pp. 2853–2858, 2016.
- [3] T. H. Tsai, C. P. Chiu, H. W. Wu, and C. C. Kuo, “Mobile device and antenna structure,” U.S. Patent 2014/0125528, 2014.
- [4] S. J. Hong, K. J. Jung, S. J. Rho, Y. B. Kwon, J. W. Lee, and D. S. Choi, “Mobile terminal,” U.S. Patent 2016/0315651, 2016.
- [5] K. L. Wong and C. Y. Tsai, “IFA-based metal-frame antenna without ground clearance for the LTE/WWAN operation in the metal-casing tablet computer,” *IEEE Transactions on Antennas and Propagation*, vol. 64, no. 1, pp. 53–60, 2016.
- [6] Y. L. Ban, Y. F. Qiang, G. Wu, H. Wang, and K. L. Wong, “Reconfigurable narrow-frame antenna for LTE/WWAN metal-rimmed smartphone applications,” *IET Microwaves, Antennas & Propagation*, vol. 10, no. 10, pp. 1092–1100, 2016.
- [7] M. Zheng, H. Wang, and Y. Hao, “Internal hexa-band folded monopole/dipole/loop antenna with four resonances for mobile device,” *IEEE Transactions on Antennas and Propagation*, vol. 60, no. 6, pp. 2880–2885, 2012.
- [8] D. Wu, S. W. Cheung, and T. I. Yuk, “A compact and low-profile loop antenna with multiband operation for ultra-thin smartphones,” *IEEE Transactions on Antennas and Propagation*, vol. 63, no. 6, pp. 2745–2750, 2015.
- [9] D. Wu, S. W. Cheung, and T. I. Yuk, “Compact 3D-loop antenna with bandwidth enhancement for WWAN/LTE mobile-phones applications,” *IET Microwaves, Antennas & Propagation*, vol. 11, no. 2, pp. 240–246, 2017.
- [10] C. C. Yong, “Apparatus for tuning multi-band frame antenna,” U.S. Patent 2015/0084817, 2015.
- [11] Y.-L. Ban, Y.-F. Qiang, Z. Chen, K. Kang, and J.-H. Guo, “A dual-loop antenna design for hepta-band WWAN/LTE metal-rimmed smartphone applications,” *IEEE Transactions on Antennas and Propagation*, vol. 63, no. 1, pp. 48–58, 2015.
- [12] M. Pascolini, R. J. Hill, J. Zavala et al., “Bezel gap antennas,” U.S. Patent 8 270 914, 2012.
- [13] D. Kwak, S. Rho, and K. Jung, “Mobile terminal,” U.S. Patent 9 431 693, 2016.
- [14] I. Poole, “LTE frequency bands and spectrum allocations,” <http://www.radio-electronics.com/>.

- [15] C. A. Balanis, *Antenna Theory Analysis and Design*, John Wiley & Sons, 2005.
- [16] K. R. Boyle and L. P. Ligthart, "Radiating and balanced mode analysis of PIFA antennas," *IEEE Transactions on Antennas and Propagation*, vol. 54, no. 1, pp. 231–237, 2006.
- [17] K. D. Katsibas, C. A. Balanis, P. A. Tirkas, and C. R. Birtcher, "Folded loop antenna for mobile hand-held units," *IEEE Transactions on Antennas and Propagation*, vol. 46, no. 2, pp. 260–266, 1998.
- [18] H. Wang, Y. Wang, J. Wu et al., "Small-size reconfigurable loop antenna for mobile phone applications," *IEEE Access*, vol. 4, pp. 5179–5186, 2016.
- [19] H. Xu, H. Wang, S. Gao et al., "A compact and low-profile loop antenna with six resonant modes for LTE smartphone," *IEEE Transactions on Antennas and Propagation*, vol. 64, no. 9, pp. 3743–3751, 2016.
- [20] H. B. Zhang, Y. L. Ban, Y. F. Qiang, J. Guo, and Z. F. Yu, "Reconfigurable loop antenna with two parasitic grounded strips for WWAN/LTE unbroken metal-rimmed smartphones," *IEEE Access*, vol. 5, pp. 4853–4858, 2017.
- [21] J. W. Lian, Y. L. Ban, Y. L. Yang, L. W. Zhang, C. Y. D. Sim, and K. Kang, "Hybrid multi-mode narrow-frame antenna for WWAN/LTE metal-rimmed smartphone applications," *IEEE Access*, vol. 4, pp. 3991–3998, 2016.
- [22] Y. Liu, Y. M. Zhou, G. F. Liu, and S. X. Gong, "Heptaband inverted-F antenna for metal-rimmed mobile phone applications," *IEEE Antennas and Wireless Propagation Letters*, vol. 15, pp. 996–999, 2016.

